Product Datasheet

HIF-2 alpha/EPAS1 Antibody (ep190b)
NB100-132

Unit Size: 0.1 ml

Aliquot and store at -20C or -80C. Avoid freeze-thaw cycles.

www.novusbio.com technical@novusbio.com

Reviews: 9 Publications: 195

Protocols, Publications, Related Products, Reviews, Research Tools and Images at:
www.novusbio.com/NB100-132

Updated 9/9/2025 v.20.1

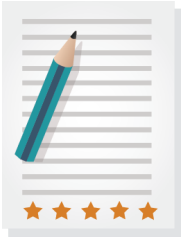

NB100-132

HIF-2 alpha/EPAS1 Antibody (ep190b)

Product Information	
Unit Size	0.1 ml
Concentration	1.0 mg/ml
Storage	Aliquot and store at -20C or -80C. Avoid freeze-thaw cycles.
Clonality	Monoclonal
Clone	ep190b
Preservative	0.05% Sodium Azide
Isotype	IgG1
Purity	Protein G purified
Buffer	PBS, 1% BSA
Target Molecular Weight	96.5 kDa

Product Description	
Description	Novus Biologicals Mouse HIF-2 alpha/EPAS1 Antibody (ep190b) (NB100-132) is a monoclonal antibody validated for use in IHC, WB, ELISA, Flow, ICC/IF, Simple Western, IP and ChIP. Anti-HIF-2 alpha/EPAS1 Antibody: Cited in 194 publications. All Novus Biologicals antibodies are covered by our 100% guarantee.
Host	Mouse
Gene ID	2034
Gene Symbol	EPAS1
Species	Human, Mouse, Rat, Bovine, Hamster
Reactivity Notes	Ability to use HIF-2 alpha/EPAS1 Antibody (ep190b) in mouse is mixed with some positive and some negative results. Use in Bovine reported in scientific literature (PMID:32054096).
Specificity/Sensitivity	This HIF-2 alpha/EPAS1 Antibody (ep190b) is specific for HIF-2 alpha/EPAS1, and does not cross-react with HIF-1 alpha.
Immunogen	The immunogen recognized by this HIF-2 alpha/EPAS1 Antibody (ep190b) maps to a region between amino acids 535-631. [UniProt# Q99814]

Product Application Details	
Applications	Western Blot, Simple Western, Immunohistochemistry-Paraffin, ELISA, Flow Cytometry, Gel Super Shift Assays, Immunocytochemistry/ Immunofluorescence, Immunohistochemistry, Immunohistochemistry-Frozen, In vivo assay, Immunoprecipitation, Chromatin Immunoprecipitation (ChIP), Gel Supershift Assay, Knockdown Validated
Recommended Dilutions	Western Blot 1 - 2 ug/mL, Simple Western 1:100, Flow Cytometry 1:400, ELISA 1:100-1:2000, Immunohistochemistry 1:150 - 1:300, Immunocytochemistry/ Immunofluorescence, Immunoprecipitation, Immunohistochemistry-Paraffin 1:150 - 1:300, Immunohistochemistry-Frozen reported in scientific literature (PMID 24973414), Gel Super Shift Assays reported in scientific literature (PMID 17404621), In vivo assay reported in scientific literature (PMID 23857308), Gel Supershift Assay, Chromatin Immunoprecipitation (ChIP), Knockdown Validated reported in scientific literature (PMID 32054096)

Application Notes	In WB, it recognizes a band at approx. 118 kDa representing HIF-2 alpha. In Simple Western only 10 - 15 uL of the recommended dilution is used per data point. See Simple Western Antibody Database for Simple Western validation: Tested in Hypoxic HeLa lysate 0.5 mg/mL, separated by Size, antibody dilution of 1:100, apparent MW was 137 kDa. Separated by Size-Wes, Sally Sue/Peggy Sue. The observed molecular weight of the protein may vary from the listed predicted molecular weight due to post translational modifications, post translation cleavages, relative charges, and other experimental factors.

Images

Simple Western: HIF-2 alpha/EPAS1 Antibody (ep190b) [NB100-132] - Lane view shows a specific band for HIF-2 alpha in 0.5 mg/mL of Hypoxic HeLa lysate. This experiment was performed under reducing conditions using the 12-230 kDa separation system.	
Western Blot: HIF-2 alpha/EPAS1 Antibody (ep190b) [NB100-132] - Analysis of HIF-2 alpha stabilization over time in 791T cells following exposure to hypoxia. Image using the HRP form of this antibody (NB100-132H). Image collected and cropped by CiteAb from the following publication (//pubmed.ncbi.nlm.nih.gov/23785417/) licensed under a CC-BY license.	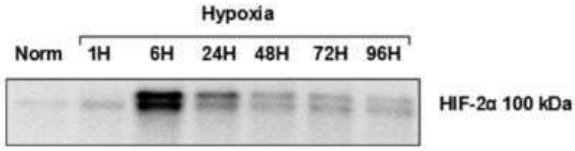
Immunohistochemistry-Paraffin: HIF-2 alpha/EPAS1 Antibody (ep190b) [NB100-132] - Analysis of HIF-2 in human cardiac myocytes using HIF-2 alpha/EPAS1 Antibody (ep190b).	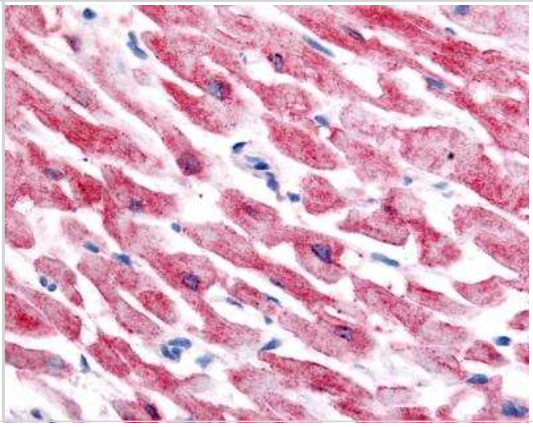

Flow Cytometry: HIF-2 alpha/EPAS1 Antibody (ep190b) [NB100-132] - HIF-2 alpha antibody was tested at 1:400 in HepG2 cells using an Alexa Fluor 488 secondary (shown in purple). M1 is defined by unstained cells.

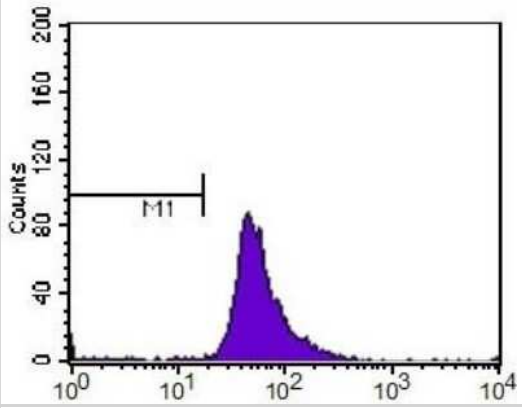

Western Blot: HIF-2 alpha/EPAS1 Antibody (ep190b) [NB100-132] - Mouse aortic endothelial cells treated (1%) or not treated (20.9%) in hypoxia for 3 hrs. Cells where also transfected with a specific siRNA against (siHIF-2) or a control siRNA (-). Western blot image submitted by a verified customer review.

Immunohistochemistry-Paraffin: HIF-2 alpha/EPAS1 Antibody (ep190b) [NB100-132] - Renal tubule specific models of Vhl deletion. Histological images of representative renal sections from 12 month old control, Pax8-CreERT2/Vhldelta/delta and Slc22a6-CreERT2/Vhldelta/delta mice (stains and antibodies as indicated, arrowheads indicate abnormal vascularization). Scale bars, 100 um. Image collected and cropped by CiteAb from the following publication (https://dx.plos.org/10.1371/journal.pone.0148055), licensed under a CC-BY license.

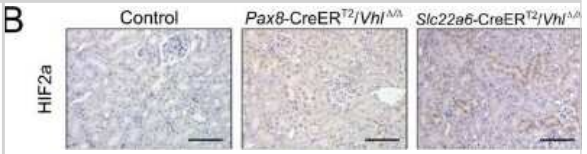

Western Blot: HIF-2 alpha/EPAS1 Antibody (ep190b) [NB100-132] - Analysis of HepG2 without Cobalt (II) Chloride (1), HepG2 with Cobalt (II) Chloride (2), HepG2 normoxic (3), HepG2 hypoxic (4), HepG2 without Cobalt (II) Chloride (5), HepG2 with Cobalt (II) Chloride (6), HepG2 normoxic (7), and HepG2 hypoxic (8) using this antibody (NB100-132) at 1 - 2 ug/mL.

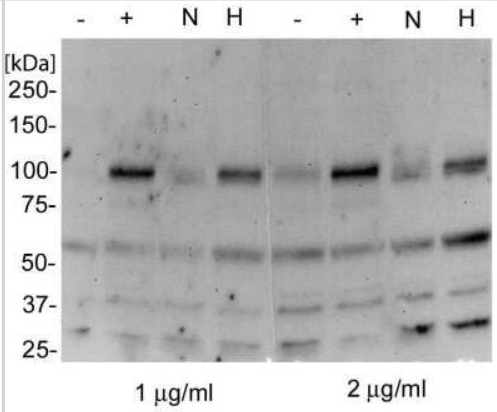

Western Blot: HIF-2 alpha/EPAS1 Antibody (ep190b) [NB100-132] - [HRP] [NB100-132H] - Analysis of HIF-2 alpha stabilization over time in HOS cells following exposure to hypoxia. Image using the HRP form of this antibody (NB100-132H). Image collected and cropped by CiteAb from the following publication (//pubmed.ncbi.nlm.nih.gov/23785417/) licensed under a CC-BY license.

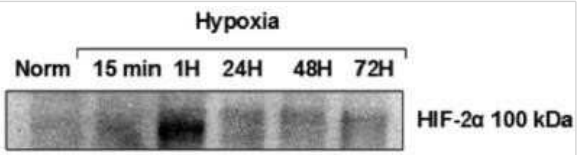

Western Blot: HIF-2 alpha/EPAS1 Antibody (ep190b) [NB100-132] - Western blot analysis and quantification of HIF-2 alpha expression in the cortex 4.5 hours after lipopolysaccharide (LPS) administration for all LPS groups and the control group (SHAM, white bar). With the exception of the vagotomy group (VGX LPS, gray bar), no significant differences to the SHAM group were found in the LPS-treated and sham-operated (SHAM+LPS, light gray bar) or vagus nerve-stimulated groups (VGX LPS+STIM, black bar). The significant increase in the VGX LPS (gray bar) group is an indicator of a hypoxic condition; * P<0.05 compared to SHAM; n=6 rats each. Data are given as the mean+/-SEM. Image collected and cropped by CiteAb from the following publication (https://jneuroinflammation.biomedcentral.com/articles/10.1186/1742-2094-9-183), licensed under a CC-BY license.

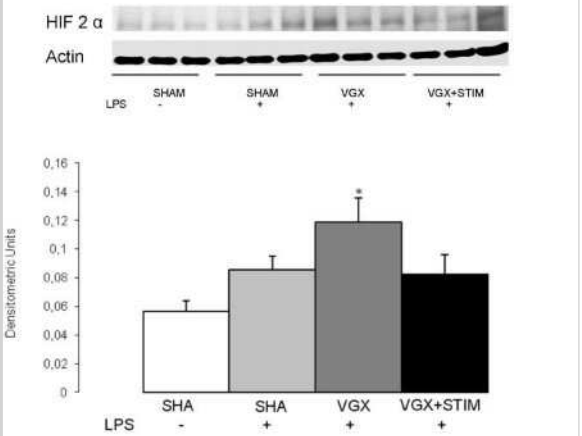

Western Blot: HIF-2 alpha/EPAS1 Antibody (ep190b) [NB100-132] - 4-OOHCPA exposure induced HIF-2 alpha/EPAS1. A: Western blot analysis of HIF-2 alpha/EPAS1 protein (118KD) and actin (43KD) in limbs at 10 min, 1, 3, 6, and 24 h after treatment with 4-OOHCPA at 0.3 ug/mL (L) 1.0 ug/mL (M) or 3.0 ug/mL (H). P represents the positive control. Image collected and cropped by CiteAb from the following publication (https://dx.plos.org/10.1371/journal.pone.0051937), licensed under a CC-BY license.

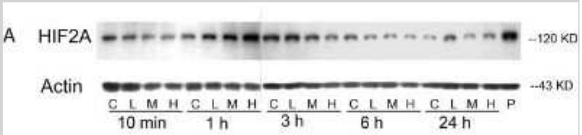

Immunohistochemistry: HIF-2 alpha/EPAS1 Antibody (ep190b) [NB100-132] - Analysis of HIF-2 alpha in human endometrium using. Donkey anti-mouse Alexa Fluor 488 secondary antibody was used. IHC image submitted by a verified customer review.

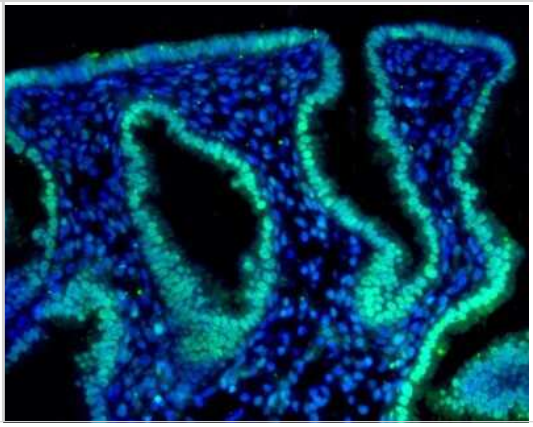

Western Blot: HIF-2 alpha/EPAS1 Antibody (ep190b) [NB100-132] - Functional role of HIF2A in the transcriptional regulation of amphiregulin (AREG) in human cardiac myocytes. Immunoblot for HIF1A or HIF2A from shRNA-transfected normoxic or hypoxic HCM. Beta-Actin (ACTb) served as a loading control. Image collected and cropped by CiteAb from the following publication (//pubmed.ncbi.nlm.nih.gov/29483579/) licensed under a CC-BY license.

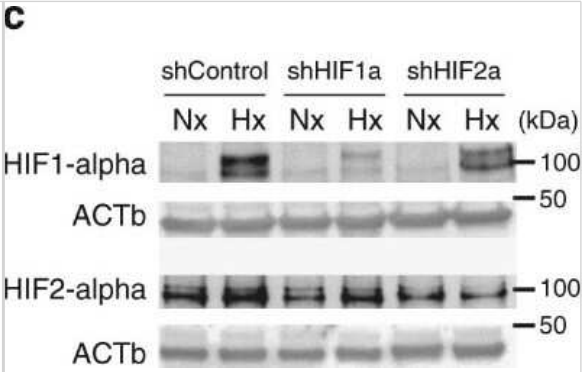

Immunohistochemistry-Paraffin: HIF-2 alpha/EPAS1 Antibody (ep190b) [NB100-132] - HIF-1α & HIF-2α IHC signals in hypoxic areas of transgenic mouse mammary tumours.A, C Hypoxyprobe (Hyp.pr.) allows visualisation of hypoxic tumour areas. B. Hypoxic peri-necrotic HIF-1α-positive cells display nuclear staining. D. HIF-2α-positive cells show cytoplasmic staining with or without appreciable nuclear staining. * necrosis. E, F. IHC staining for HIF-1α on MCF-7 breast cancer cells grown under control (E) & hypoxic (F) conditions respectively. G, H. Control (G) & hypoxic (H) MCF-7 cells IHC stained for HIF-2α. 20x obj. Insets show magnification of the boxed area. Size bars 50 µm. Image collected & cropped by CiteAb from the following publication (https://dx.plos.org/10.1371/journal.pone.0125771), licensed under a CC-BY license. Not internally tested by Novus Biologicals.

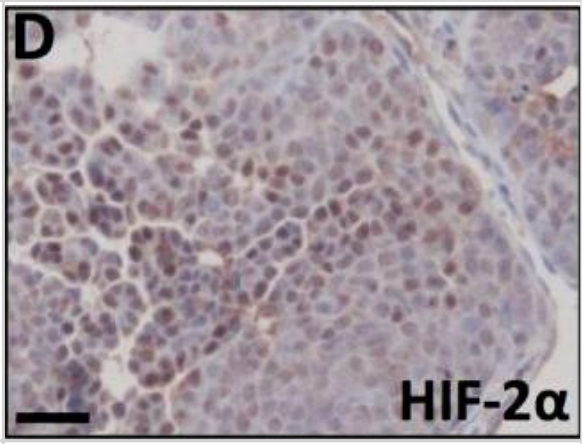

Immunohistochemistry: HIF-2 alpha/EPAS1 Antibody (ep190b) [NB100-132] - HIF-2α expression in the involuting mammary gland.Inserts are enlargements of the indicated areas. Size bars: 50 µm, 40x obj was used in all micrographs. A. In the early involuting gland, the morphology resembles the lactating gland & the basement membrane is evident at this stage. B-D. As tissue remodelling proceeds during involution, the collagen layer becomes unstructured. E-H. HIF-2α-positive cells were detected at all studied stages of involution. I-L. Macrophage infiltration (F4/80 positive) was first evident at the fifth day of involution (J) & increased with time (K, L). Image collected & cropped by CiteAb from the following publication (https://dx.plos.org/10.1371/journal.pone.0125771), licensed under a CC-BY license. Not internally tested by Novus Biologicals.

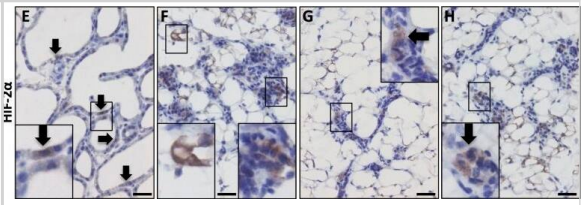

Western Blot: HIF-2 alpha/EPAS1 Antibody (ep190b) [NB100-132] - Oxygen concentration-dependence of dioxygenase inhibition.A. HIF1α, HIF2α, & H3K9me2 abundance by western blotting in shRNA1 & shRNA2 cells incubated in 21%, 10%, or 2% oxygen for 72 h. Actin & total H3 serve as loading controls. B. HIF1α, HIF2α, & H3K9me2 abundance by western blotting in SDHC knockout iMEFs incubated in 21%, 10%, or 2% oxygen for 72 h. iMEFs were treated with 1 µM TAM for 7 d prior to analysis. (C-D) Rescue of succinate inhibition of JMHD & PHD inhibition using 0.25 mM octyl-α-ketoglutarate (octyl-α-KG) in SDHB knockdown HEK293 cells & SDHC knockout mouse iMEFs. Image collected & cropped by CiteAb from the following publication (https://dx.plos.org/10.1371/journal.pone.0127471), licensed under a CC-BY license. Not internally tested by Novus Biologicals.

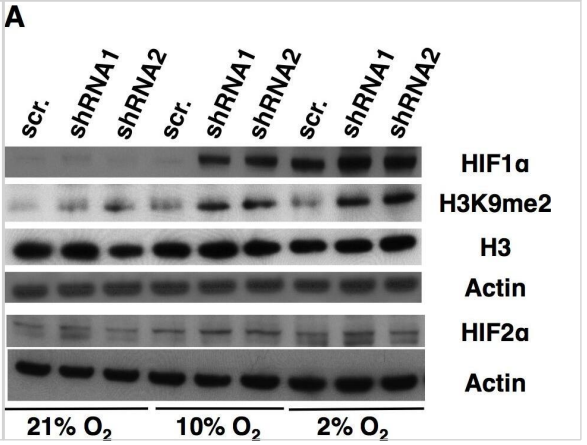

Immunohistochemistry-Paraffin: HIF-2 alpha/EPAS1 Antibody (ep190b) [NB100-132] - Lactating mammary gland.Smaller panels display enlargements of the indicated areas. Size bars: 50 µm, 40x obj was used for all micrographs. A. Collagen I IHC allows visualisation of the basement membrane surrounding the dilated ducts. B. HIF-1α was not detected in the epithelial cells of the lactating gland (compare with Fig 1). C. Macrophage infiltration was sparse in the lactating mammary gland as judged by F4/80 IHC. D. A subset of cuboidal luminal epithelial cells was distinctively positive for HIF-2α. E. The percentage of HIF-2α-positive out of total luminal epithelial cells was counted in sections from three mice. Image collected & cropped by CiteAb from the following publication (https://dx.plos.org/10.1371/journal.pone.0125771), licensed under a CC-BY license. Not internally tested by Novus Biologicals.

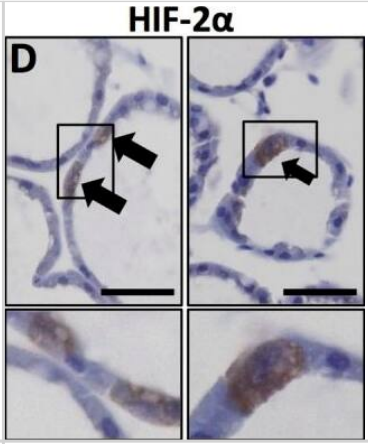

Immunohistochemistry: HIF-2 alpha/EPAS1 Antibody (ep190b) [NB100-132] - Mainly CK14-positive, but not CK8-positive, mammary epithelial cells are HIF-2α positive at day 14 post weaning.Left panels 20x & right 40x objective. Size bars 50 µm. a, A, b & B. Double IHC for HIF-2α (green) & CK8 (a, A) & CK14 (b, B), respectively (red), reveal that few (if any) CK8-positive luminal cells are HIF-2α positive. Numerous CK14-expressing cells, which include basal & stem/progenitor cells, were positive for HIF-2α. c, C. F4/80 IHC was performed on an adjacent tissue section detect macrophages. Image collected & cropped by CiteAb from the following publication (https://dx.plos.org/10.1371/journal.pone.0125771), licensed under a CC-BY license. Not internally tested by Novus Biologicals.

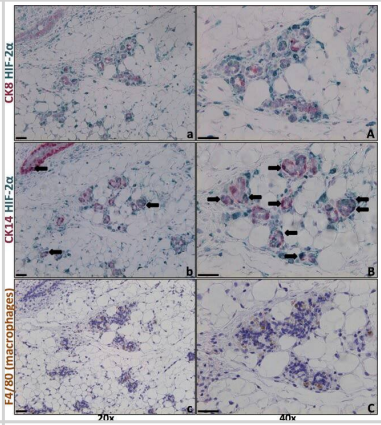

Immunohistochemistry: HIF-2 alpha/EPAS1 Antibody (ep190b) [NB100-132] - Renal tubule specific models of Vhl deletion.(A) PCR analysis of recombination at the Vhl locus in the kidneys of mice with combinations of Pax8-CreERT2, Slc22a6-CreERT2 & the Vhl floxed (fl) & wild-type (+) alleles. The positions of the bands representing the Vhl floxed, wild type (Wt) & recombined (Δ) alleles are indicated. (B) Histological images of representative renal sections from 12 month old control, Pax8-CreERT2/VhlΔ/Δ & Slc22a6-CreERT2/VhlΔ/Δ mice (stains & antibodies as indicated, arrowheads indicate abnormal vascularisation). Scale bars, 100µm. Image collected & cropped by CiteAb from the following publication (https://pubmed.ncbi.nlm.nih.gov/26866916), licensed under a CC-BY license. Not internally tested by Novus Biologicals.

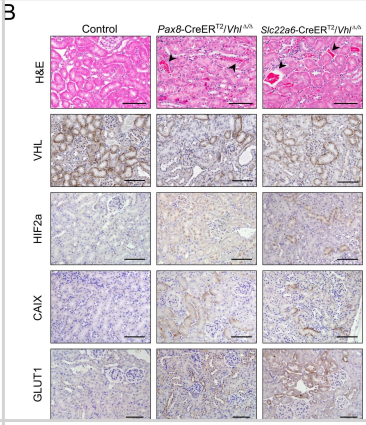

Immunohistochemistry-Paraffin: HIF-2 alpha/EPAS1 Antibody (ep190b) [NB100-132] - HIF1α & H3K9me2 accumulation & 5-hydroxy-methyl-2'-deoxycytidine (5hmdC) depletion in PGL specimens compared to controls.Normal ganglia 1 (NG1), normal ganglia 2 (NG2) & IDH-mutant (IDH). Sporadic PGL (Spo. PGL). A. HIF1α staining. B. HIF2α staining. C. H3K9me2 staining. Arrows indicate H3K9me2 staining in nuclei of neurons or chief cells. D. 5hmdC staining. Arrows indicate 5hmdC staining in the nuclei of neurons & chief cells. Image collected & cropped by CiteAb from the following publication (https://dx.plos.org/10.1371/journal.pone.0127471), licensed under a CC-BY license. Not internally tested by Novus Biologicals.

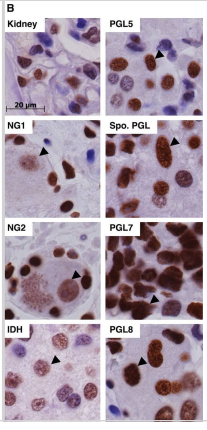

Immunohistochemistry: HIF-2 alpha/EPAS1 Antibody (ep190b) [NB100-132] - Localization of HIF2A immunoreactivity in limbs.HIF-2A reactivity was detected in control limbs at 1 & 3 h in the apical ectodermal ridge, interdigital area (I.R.) & developing cartilaginous anlagen (Digits). 4-OOHCPA exposure increased HIF2A immunoreactivity in the apical ectodermal ridge & interdigital regions (I.R.) at 3 h. No differences were observed between control & drug-treated limbs after 6 h or 24 h of culture. Four separate replicates were done. Image collected & cropped by CiteAb from the following publication (https://dx.plos.org/10.1371/journal.pone.0051937), licensed under a CC-BY license. Not internally tested by Novus Biologicals.

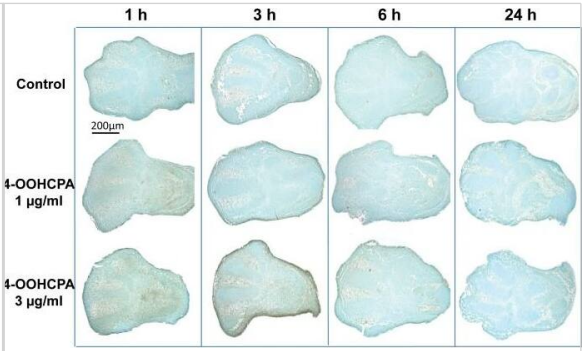

Western Blot: HIF-2 alpha/EPAS1 Antibody (ep190b) [NB100-132] - Hypoxic repression of ER-α is dependent on HIF-1α. a Representative western blots of HIF-1α, HIF-2α & β-actin protein in ten ER-positive cell lines grown at normoxia or hypoxia (1% O2, 24 h). b qPCR analysis of HIF1A mRNA levels in MCF7, BT474, T47D & ZR75B transfected with shScramble or shHIF1A. Relative HIF1A mRNA levels normalized to TBP. (Change in HIF1A levels: *p < 0.0001 MCF7, *p = 0.012 BT474, *p < 0.0001 T47D, *p = 0.0046 ZR75B). c Representative western blots of HIF-1α, ER-α & β-actin protein from MCF7, BT474, T47D & ZR75B with either shScramble or shHIF1A at normoxia & hypoxia (1% O2, 24 h). β-actin is used as a loading control. d Representative western blot of HIF-1α, ER-α & β-actin protein from MCF7, BT474, T47D & ZR75B with or without the transfection of stabilized HIF-1α (HIF-1αODD) Image collected & cropped by CiteAb from the following publication (https://pubmed.ncbi.nlm.nih.gov/28320353), licensed under a CC-BY license. Not internally tested by Novus Biologicals.

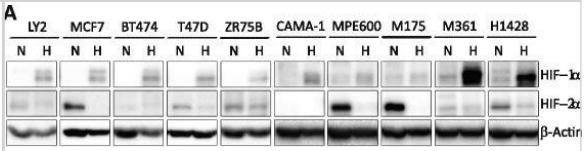

Immunohistochemistry: HIF-2 alpha/EPAS1 Antibody (ep190b) [NB100-132] - HIF-1α & HIF-2α expression in the virgin mammary gland.A. Virgin mammary glands (30 & 70 days old) showed no conspicuous basal membrane, as visualised by collagen IV IHC (a, b). There was also no detectable expression of HIF-2α in the epithelial cells (c, d). Macrophages (F4/80 positive) were few. In panel c, a single HIF-2α-positive cell was detected, & the adjacent F4/80 IHC section (e) suggested that this cell is a macrophage. B. Expression of HIF-1α in mammary epithelium in the 70-day-old virgin mouse. Top panel, orientation slide with haematoxylin (HTX) staining, 20x obj. *lymph node. Panels b, d, f. Cross-section of a developing duct close to the invading tip at a stage where the lumen is not yet evacuated, 40x obj. Panels c, e, g. Cross-section of a less mature part of a duct, 40x obj. CK14-expressing cells (marker of basal mammary epithelial cells) can be seen in more than one cell layer (panels b & c, arrow-head). At this stage, the lumen is evacuated, but there is still more than one layer of epithelial cells. HIF-1α IHC on the adjacent sections (panels d, e) showing nuclear expression in non-basal epithelial cells (highlighted by red arrows). Basal (CK14 positive) epithelial cells did not express HIF-1α (black arrows). Mammary epithelial expression of HIF-2α was not detected at these developmental stages. Size bars: 50 µm. Image collected & cropped by CiteAb from the following publication (https://dx.plos.org/10.1371/journal.pone.0125771), licensed under a CC-BY license. Not internally tested by Novus Biologicals.

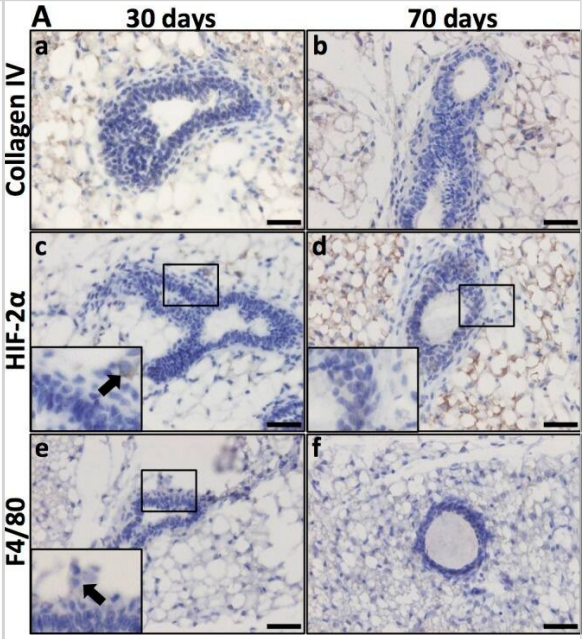

Western Blot: HIF-2 alpha/EPAS1 Antibody (ep190b) [NB100-132] - HIF2α inhibitor 76 suppressed CoCl2-induced immature phenotypic characteristics of BCSCs(A) The inhibitory effect of small molecule HIF2α inhibitor 76 for 24h (10 μM for 4T1 cells; 25 μM for Hs578T cells) on CoCl2-induced expression of HIF2α was assessed in both 4T1 & Hs578T cells by western blot analysis. (B) HIF2α inhibitor 76 inhibited primary (with HIF2α inhibitor 76 daily treatment) & second sphere formation (without additional HIF2α inhibitor 76 treatment) in both 4T1 & Hs578T cells. The sizes of spheres greater than 100 μm were enumerated, with a representative image of a tumor-sphere shown. The data represents an average of three independent experiments. (C) Treatment of 4T1 & Hs578T cells with HIF2α inhibitor 76 for 24 h led to a decrease in the percentage of CD44+/CD24−-positive cells as a proportion of total cancer cells. (D) 4T1 & Hs578T cells treated with CoCl2 (100 μM) for 24h & HIF2α inhibitor 76 for 24h (10 μM for 4T1 cells; 25 μM for Hs578T cells) either alone or together were evaluated for the expression levels of stem cell markers c-Myc, Klf4, Oct4, & Nanog by Real-time PCR. Abbreviations: TSFE, Tumor sphere-forming efficiency. β-actin was used as the internal control. The results represent the mean ± SD from three independent experiments. Image collected & cropped by CiteAb from the following publication (https://www.oncotarget.com/lookup/doi/10.18632/oncotarget.9846), licensed under a CC-BY license. Not internally tested by Novus Biologicals.

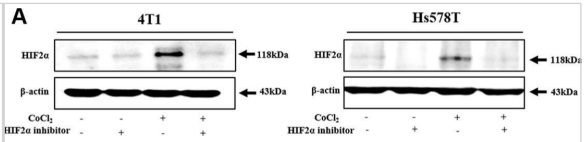

Western Blot: HIF-2 alpha/EPAS1 Antibody (ep190b) [NB100-132] - Phd2 deletion leads to activation of the Akt–mTOR pathway. a RPPA analysis of tumors with homozygous deletion of Phd2. Tumor tissues from Tyr::CreER; BRafV600E; Phd2−/− or Tyr::CreER; BRafV600E mice were processed & analyzed by RPPA assays. The analyses identified proteins that were significantly changed in mouse melanomas compared to nevi. b Activation of Akt–mTOR pathway after phd2 deletion. Tumor tissues were processed & western blots showed stabilization of HIF-1α & HIF-2α proteins after Phd2 depletion. Increased phosphorylation of Akt, 4EBP1 & S6K was observed in tumors from Tyr::CreER; BRafV600E; Phd2−/− compared with those of Tyr::CreER; BRafV600E mice. c Re-expression of Phd2 inhibits the Akt–mTOR pathway. A BRafV600E; Phd2−/− mouse melanoma cell line was established from melanomas in Tyr::CreER; BRafCA; Phd2lox/lox mice. Phd2 was ectopically reintroduced in these tumor cells. Western blot analysis showed that degradation of HIF-1α & HIF-2α proteins with decreased expression of VEGFR2 decreased phosphorylation of Akt, 4EBP1 & S6K. d Pharmacological inhibition (FM19G11) of HIF pathway in BRafV600E; Phd2−/− melanoma cells. A similar but more pronounced inhibition of the Akt–mTOR pathway was observed using the HIF inhibitor. β-Actin was used as a loading control. Results are representative of three independent experiments Image collected & cropped by CiteAb from the following publication (https://pubmed.ncbi.nlm.nih.gov/30575721), licensed under a CC-BY license. Not internally tested by Novus Biologicals.

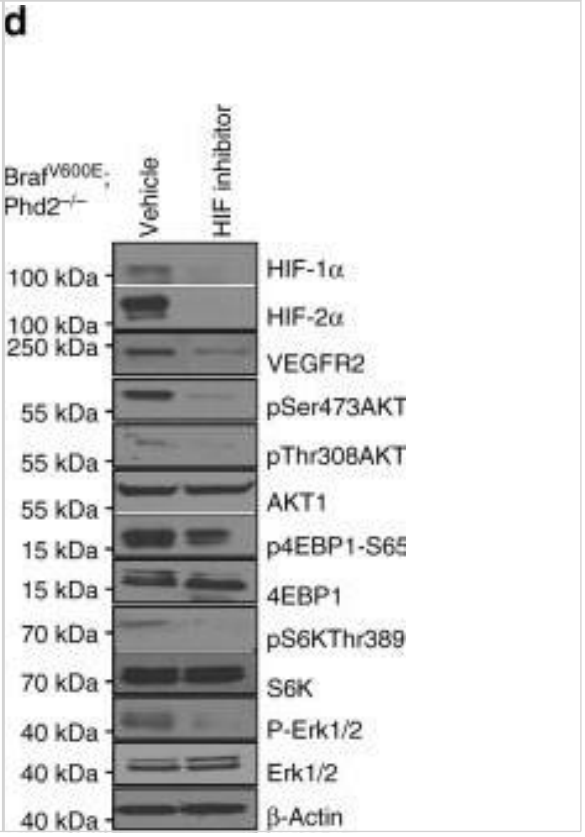

Western Blot: HIF-2 alpha/EPAS1 Antibody (ep190b) [NB100-132] - BAY 87-2243 inhibits hypoxia-inducible factor (HIF-1α) & HIF-2α protein accumulation in hypoxic H460 cells H460 under hypoxia but has no effect on HIF-1α protein levels induced by hypoxia mimetics & has no effect on prolyl hydroxylase 2 (PHD2) activity. (A, B) H460 cells were cultured for 16 h under normoxia or hypoxia (1% pO2) in the absence or presence of various concentrations of BAY 87-2243. HIF-1α (A) & HIF-2α (B) protein levels were assessed by Western Blot in whole cell extracts. β-actin was used as a loading control. (C) H460 cells were cultured for 16 h under normoxia with the PHDs desferrioxamine (DFO) & CoCl2 plus/minus BAY 87-2243 before the HIF1α protein levels in cellular extracts were quantified by Western Blot. β-actin was used to as a loading control. (D) Effect of BAY 87-2243 on the recombinant PHD2-mediated hydroxylation of HIF-1α peptide over time was measured in a biochemical assay. Hydoxylated peptide was quantified after incubation with purified VBC complex labeled with europium using fluorescence as a readout. The known PHD inhibitor N-oxalylglycine served as a positive control. Image collected & cropped by CiteAb from the following publication (https://pubmed.ncbi.nlm.nih.gov/24403227), licensed under a CC-BY license. Not internally tested by Novus Biologicals.

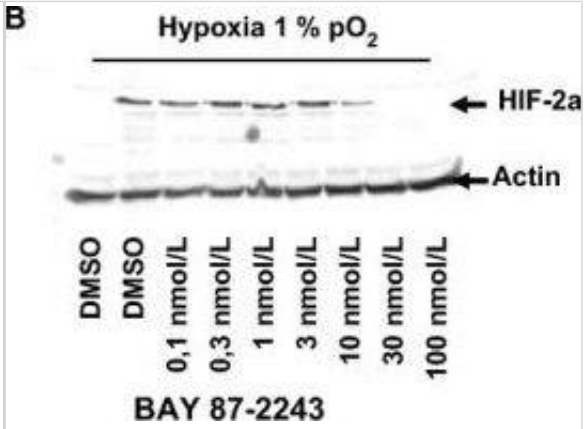

Western Blot: HIF-2 alpha/EPAS1 Antibody (ep190b) [NB100-132] - Cytosol-restricted Acss2 is enzymatically active.(A) Acetylation of ectopic HA-tagged HIF-2α detected by immunoblotting (IB) with anti-HA or anti-acetylated lysine antibodies following immunoprecipitation (IP) with anti-HA antibody in stably transformed HT1080 cells with knockdown of endogenous Acss2 & rescue with ectopic wild-type (WT) or cytosol-restricted mutant (CYT) Acss2 without or with an SV40 nuclear localization signal fused to the amino terminus. Studies were performed under hypoxia, low glucose, or acetate exposure for the indicated periods. (B) Acetate-dependent lipid synthesis measured by 14C-acetate incorporation in HT1080 stably-transformed cells producing control or Acss2 shRNA downstream of a luciferase cDNA cassette & expressing ectopic control, WT, CYT, SV40-WT, or SV40-CYT Acss2. Cells were incubated under (A) control, (B) hypoxic, or (C) low glucose conditions for 48 hr with labeling performed during the last 24 hr. Comparison of samples within a given condition was made by one-way ANOVA followed by Dunnett's multiple comparisons test using control shRNA knockdown/control rescue as reference with decreased samples noted (*, P<0.05). All values are means with SD. Image collected & cropped by CiteAb from the following publication (https://dx.plos.org/10.1371/journal.pone.0190241), licensed under a CC0-1.0 license. Not internally tested by Novus Biologicals.

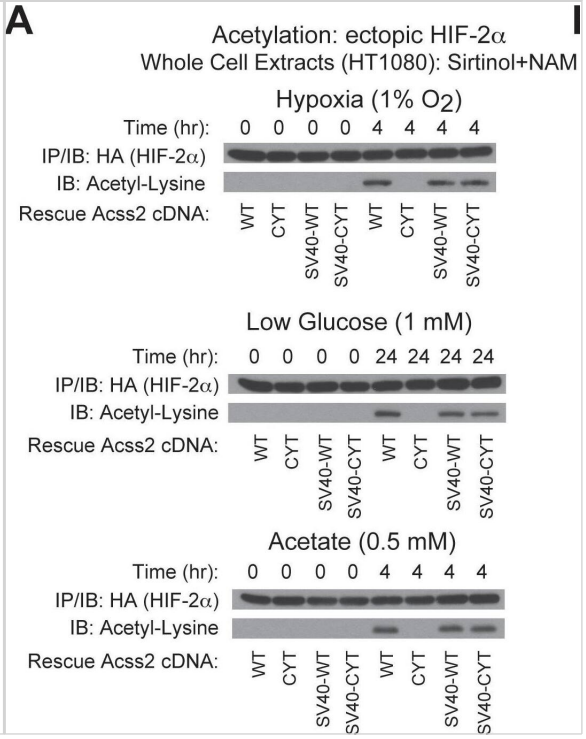

Western Blot: HIF-2 alpha/EPAS1 Antibody (ep190b) [NB100-132] - In vitro effects of diclofenac on proliferation & MYC expression in the human melanoma cell line MelIm.The human melanoma cell line MelIm was incubated with different concentrations of diclofenac (A), aspirin (ASA, B), & NS-398 (C), respectively, & proliferation was determined after 24 h. Results represent the mean +/− standard deviation of 12 (diclofenac) & 3 (ASA, NS-398) independent experiments, respectively. (D) MelIm were incubated for 24 h with or without diclofenac. Apoptotic cells were stained with Annexin-V-FITC/ 7-AAD & analyzed by flow cytometry. Results represent the mean +/− standard deviation of 3 independent experiments. (E-G) MYC, STAT3, HIF1a & HIF2a protein expression were determined in cell lysates of MelIm incubated for 2 or 24 h with or without diclofenac (E,F) or ASA (G). The effect of diclofenac on MYC promoter activity was determined by transient transfection of a 2632-bp MYC promoter fragment (H). MelIm were transfected in 6-well-plates & diclofenac was added after 5 h. Luciferase activity was determined 24 h after transfection. Results represent the mean +/− standard deviation of 3 independent experiments. Image collected & cropped by CiteAb from the following publication (https://dx.plos.org/10.1371/journal.pone.0066987), licensed under a CC-BY license. Not internally tested by Novus Biologicals.

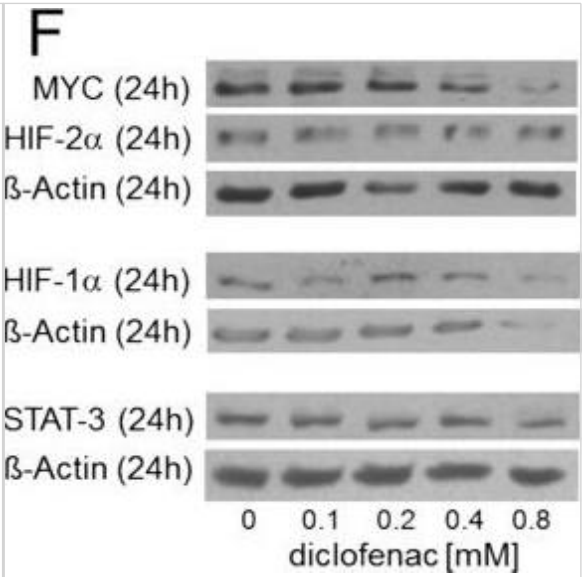

Western Blot: HIF-2 alpha/EPAS1 Antibody (ep190b) [NB100-132] - Phd2 deletion leads to activation of the Akt–mTOR pathway. a RPPA analysis of tumors with homozygous deletion of Phd2. Tumor tissues from Tyr::CreER; BRafV600E; Phd2−/− or Tyr::CreER; BRafV600E mice were processed & analyzed by RPPA assays. The analyses identified proteins that were significantly changed in mouse melanomas compared to nevi. b Activation of Akt–mTOR pathway after phd2 deletion. Tumor tissues were processed & western blots showed stabilization of HIF-1α & HIF-2α proteins after Phd2 depletion. Increased phosphorylation of Akt, 4EBP1 & S6K was observed in tumors from Tyr::CreER; BRafV600E; Phd2−/− compared with those of Tyr::CreER; BRafV600E mice. c Re-expression of Phd2 inhibits the Akt–mTOR pathway. A BRafV600E; Phd2−/− mouse melanoma cell line was established from melanomas in Tyr::CreER; BRafCA; Phd2lox/lox mice. Phd2 was ectopically reintroduced in these tumor cells. Western blot analysis showed that degradation of HIF-1α & HIF-2α proteins with decreased expression of VEGFR2 decreased phosphorylation of Akt, 4EBP1 & S6K. d Pharmacological inhibition (FM19G11) of HIF pathway in BRafV600E; Phd2−/− melanoma cells. A similar but more pronounced inhibition of the Akt–mTOR pathway was observed using the HIF inhibitor. β-Actin was used as a loading control. Results are representative of three independent experiments Image collected & cropped by CiteAb from the following publication (https://pubmed.ncbi.nlm.nih.gov/30575721), licensed under a CC-BY license. Not internally tested by Novus Biologicals.

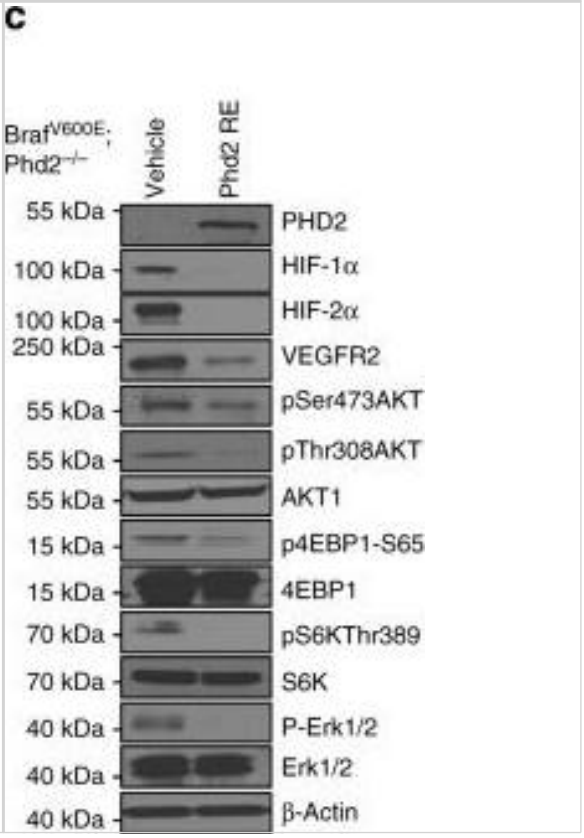

Western Blot: HIF-2 alpha/EPAS1 Antibody (ep190b) [NB100-132] - Phd2 deletion leads to activation of the Akt–mTOR pathway. a RPPA analysis of tumors with homozygous deletion of Phd2. Tumor tissues from Tyr::CreER; BRafV600E; Phd2−/− or Tyr::CreER; BRafV600E mice were processed & analyzed by RPPA assays. The analyses identified proteins that were significantly changed in mouse melanomas compared to nevi. b Activation of Akt–mTOR pathway after phd2 deletion. Tumor tissues were processed & western blots showed stabilization of HIF-1α & HIF-2α proteins after Phd2 depletion. Increased phosphorylation of Akt, 4EBP1 & S6K was observed in tumors from Tyr::CreER; BRafV600E; Phd2−/− compared with those of Tyr::CreER; BRafV600E mice. c Re-expression of Phd2 inhibits the Akt–mTOR pathway. A BRafV600E; Phd2−/− mouse melanoma cell line was established from melanomas in Tyr::CreER; BRafCA; Phd2lox/lox mice. Phd2 was ectopically reintroduced in these tumor cells. Western blot analysis showed that degradation of HIF-1α & HIF-2α proteins with decreased expression of VEGFR2 decreased phosphorylation of Akt, 4EBP1 & S6K. d Pharmacological inhibition (FM19G11) of HIF pathway in BRafV600E; Phd2−/− melanoma cells. A similar but more pronounced inhibition of the Akt–mTOR pathway was observed using the HIF inhibitor. β-Actin was used as a loading control. Results are representative of three independent experiments Image collected & cropped by CiteAb from the following publication (https://pubmed.ncbi.nlm.nih.gov/30575721), licensed under a CC-BY license. Not internally tested by Novus Biologicals.

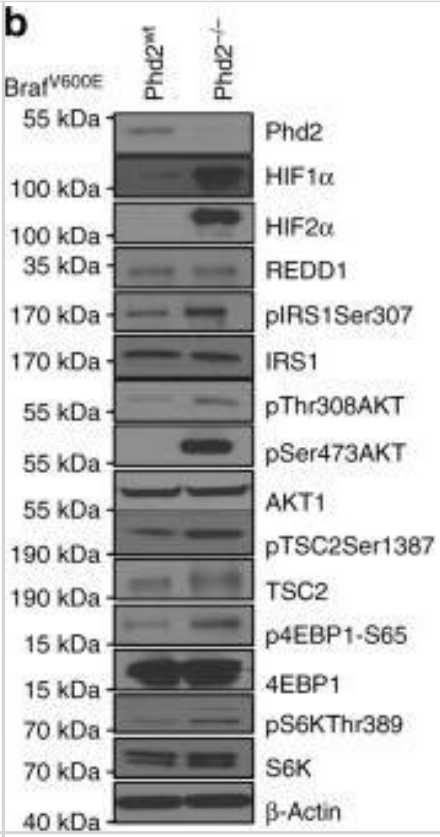

Immunohistochemistry: HIF-2 alpha/EPAS1 Antibody (ep190b) [NB100-132] - In-vivo lentiviral delivery of Cre-recombinase to renal tubular epithelium results in recombination of target genes.(a) Diagram of pCCIE lentiviral construct. Cre, Cre-recombinase; IRES, internal ribosome entry site; GFP, Green fluorescent protein. (b) Anti-VHL, HIF1a & GAPDH immunoblots of renal cortical protein lysates from Vhlwt/wt & Vhlfl/fl mice intrarenally injected with CCIE. Samples were collected 12 months post infection with each column representing an individual mouse. Blots were cropped to improve clarity, full-length blots are presented in Supplementary Fig. S3a. (c) Histological images of renal sections from Vhlwt/wt & Vhlfl/fl mice intrarenally injected with CCIE at 12 months post injection (stains & antibodies as indicated). Scale bars, 100 μm. Image collected & cropped by CiteAb from the following publication (https://pubmed.ncbi.nlm.nih.gov/26046460), licensed under a CC-BY license. Not internally tested by Novus Biologicals.

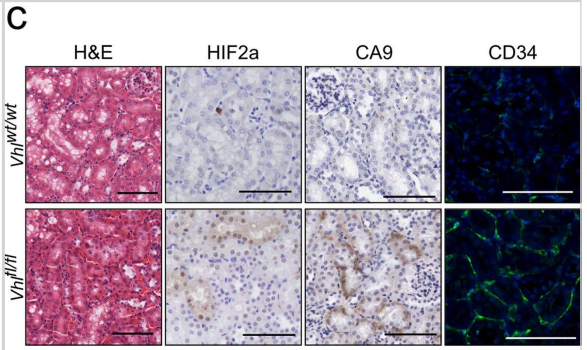

Immunohistochemistry-Paraffin: HIF-2 alpha/EPAS1 Antibody (ep190b) [NB100-132] - HIF-1α & HIF-2α expression in the virgin mammary gland.A. Virgin mammary glands (30 & 70 days old) showed no conspicuous basal membrane, as visualised by collagen IV IHC (a, b). There was also no detectable expression of HIF-2α in the epithelial cells (c, d). Macrophages (F4/80 positive) were few. In panel c, a single HIF-2α-positive cell was detected, & the adjacent F4/80 IHC section (e) suggested that this cell is a macrophage. B. Expression of HIF-1α in mammary epithelium in the 70-day-old virgin mouse. Top panel, orientation slide with haematoxylin (HTX) staining, 20x obj. *lymph node. Panels b, d, f. Cross-section of a developing duct close to the invading tip at a stage where the lumen is not yet evacuated, 40x obj. Panels c, e, g. Cross-section of a less mature part of a duct, 40x obj. CK14-expressing cells (marker of basal mammary epithelial cells) can be seen in more than one cell layer (panels b & c, arrow-head). At this stage, the lumen is evacuated, but there is still more than one layer of epithelial cells. HIF-1α IHC on the adjacent sections (panels d, e) showing nuclear expression in non-basal epithelial cells (highlighted by red arrows). Basal (CK14 positive) epithelial cells did not express HIF-1α (black arrows). Mammary epithelial expression of HIF-2α was not detected at these developmental stages. Size bars: 50 µm. Image collected & cropped by CiteAb from the following publication (https://dx.plos.org/10.1371/journal.pone.0125771), licensed under a CC-BY license. Not internally tested by Novus Biologicals.

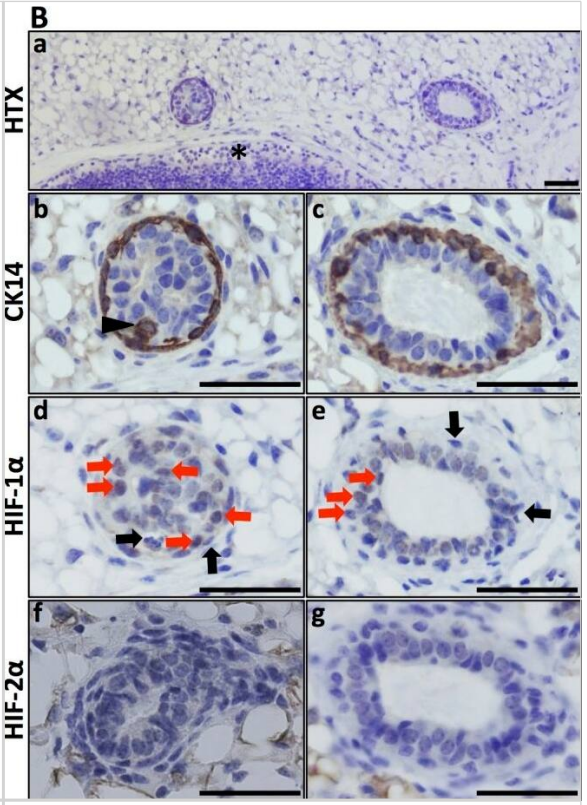

Hypoxia inducible factor (HIF)□2α is expressed in trunk neural crest cells. A,C, Immunostaining of HIF□2α in sections from trunk axial level of wild□type chick embryos at HH11, A, HH13, B, and HH18, C. Arrow denotes ventrally migrating HIF□2α positive cells. D, Co□immunostaining of HIF□2α and HNK1 (marker of migrating neural crest) in sections from trunk axial level of wild□type HH18 chick embryos. Arrows denote migrating cells double positive for the two proteins. E, Sections of HH13 wild□type embryo immunostained with DAPI for visualization of nuclei and secondary antibody only (donkey anti□rabbit Alexa Fluor□546). F, Western blot analysis for detection of HIF□2α protein at 21% and 1% O2 following siRNA mediated knockdown of HIF□1α or HIF□2α. DIP treated cells were used as a positive control and SDHA as loading control. Lanes between 21% and 1% siCTRL were removed from this figure, indicated by the black line. G, Immunohistochemical staining for HIF□2α in sections of SK□N□BE(2)c neuroblastoma cells cultured at 21% or 1% O2. H, Schematic of where oxygen measurements were performed. I, Oxygen saturation in the trunk of chick embryos during development measured ex ovo using microsensor technique. Error bars represent SEM, n ≥ 3 biologically independent replicates for each time point Image collected and cropped by CiteAb from the following open publication (https://pubmed.ncbi.nlm.nih.gov/32940375), licensed under a CC-BY license. Not internally tested by Novus Biologicals.

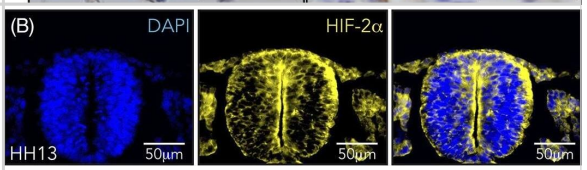

Hypoxia inducible factor (HIF)□2α is expressed in trunk neural crest cells. A,C, Immunostaining of HIF□2α in sections from trunk axial level of wild□type chick embryos at HH11, A, HH13, B, and HH18, C. Arrow denotes ventrally migrating HIF□2α positive cells. D, Co□immunostaining of HIF□2α and HNK1 (marker of migrating neural crest) in sections from trunk axial level of wild□type HH18 chick embryos. Arrows denote migrating cells double positive for the two proteins. E, Sections of HH13 wild□type embryo immunostained with DAPI for visualization of nuclei and secondary antibody only (donkey anti□rabbit Alexa Fluor□546). F, Western blot analysis for detection of HIF□2α protein at 21% and 1% O2 following siRNA mediated knockdown of HIF□1α or HIF□2α. DIP treated cells were used as a positive control and SDHA as loading control. Lanes between 21% and 1% siCTRL were removed from this figure, indicated by the black line. G, Immunohistochemical staining for HIF□2α in sections of SK□N□BE(2)c neuroblastoma cells cultured at 21% or 1% O2. H, Schematic of where oxygen measurements were performed. I, Oxygen saturation in the trunk of chick embryos during development measured ex ovo using microsensor technique. Error bars represent SEM, n ≥ 3 biologically independent replicates for each time point Image collected and cropped by CiteAb from the following open publication (https://pubmed.ncbi.nlm.nih.gov/32940375), licensed under a CC-BY license. Not internally tested by Novus Biologicals.

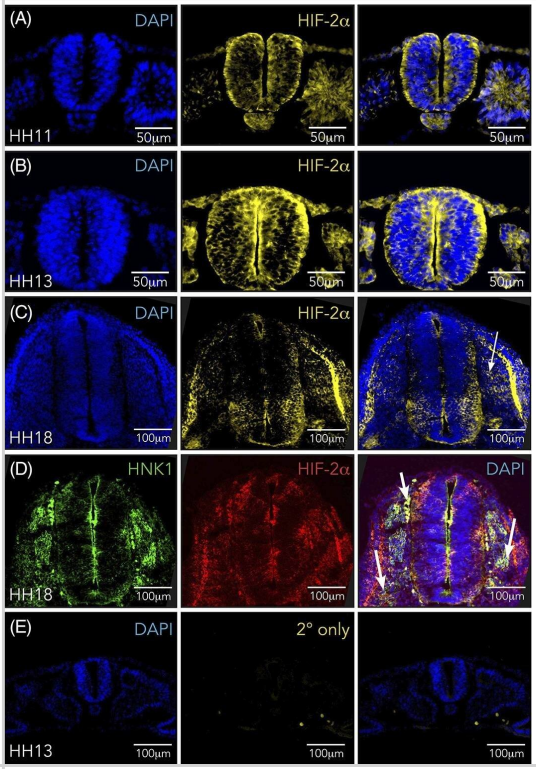

Hypoxia inducible factor (HIF)□2α is expressed in trunk neural crest cells. A,C, Immunostaining of HIF□2α in sections from trunk axial level of wild□type chick embryos at HH11, A, HH13, B, and HH18, C. Arrow denotes ventrally migrating HIF□2α positive cells. D, Co□immunostaining of HIF□2α and HNK1 (marker of migrating neural crest) in sections from trunk axial level of wild□type HH18 chick embryos. Arrows denote migrating cells double positive for the two proteins. E, Sections of HH13 wild□type embryo immunostained with DAPI for visualization of nuclei and secondary antibody only (donkey anti□rabbit Alexa Fluor□546). F, Western blot analysis for detection of HIF□2α protein at 21% and 1% O2 following siRNA mediated knockdown of HIF□1α or HIF□2α. DIP treated cells were used as a positive control and SDHA as loading control. Lanes between 21% and 1% siCTRL were removed from this figure, indicated by the black line. G, Immunohistochemical staining for HIF□2α in sections of SK□N□BE(2)c neuroblastoma cells cultured at 21% or 1% O2. H, Schematic of where oxygen measurements were performed. I, Oxygen saturation in the trunk of chick embryos during development measured ex ovo using microsensor technique. Error bars represent SEM, n ≥ 3 biologically independent replicates for each time point Image collected and cropped by CiteAb from the following open publication (https://pubmed.ncbi.nlm.nih.gov/32940375), licensed under a CC-BY license. Not internally tested by Novus Biologicals.

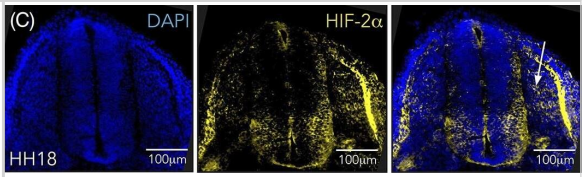

Hypoxia inducible factor (HIF)□2α affects proliferation and self□renewal capacity. A□D, Embryo sections from trunk axial level. Proliferating EdU + cells are green and electroporated cells (morpholinos, A; pCI□CTRL and pCI□EPAS1, C) are red. DAPI counterstains nuclei. Only construct targeted neural crest cells (above and outside of dotted line) were quantified (n = 82 [5′□mispair morpholino] and n = 303 [EPAS1 morpholino], B); n = 211 (pCI□CTRL) and n = 139 (pCI□EPAS1), D. Statistical significance calculated using one□way analysis of variance (ANOVA). E, Relative mRNA expression of EPAS1 in crestosphere cells established from cranial or trunk axial level measured by qRT□PCR. Expression is presented as mean of n = 4 (cranial) or n = 3 (trunk) biological replicates and error bars represent SEM. Statistical significance calculated using two□sided student's t test. F,G, Primary sphere assay of crestospheres established from embryos previously electroporated in ovo with non□ (CTRL) or EPAS1 (EPAS1.1, F, EPAS1.2, G, targeting gRNAs. One cell/well, n = 10 wells/group). Number of spheres were manually counted after 1 week. Statistical significance was calculated by one□way ANOVA. H, Size of spheres formed in, G. Manual measurements using the ImageJ software to convert to factual unit (μm). Statistical significance was determined by one□way ANOVA. Inserted photographs of representative spheres from each group Image collected and cropped by CiteAb from the following open publication (https://pubmed.ncbi.nlm.nih.gov/32940375), licensed under a CC-BY license. Not internally tested by Novus Biologicals.

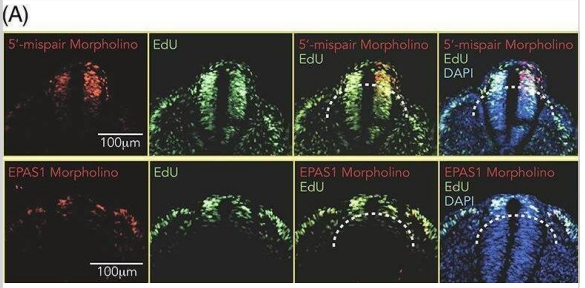

Hypoxia inducible factor (HIF)□2α is expressed in trunk neural crest cells. A,C, Immunostaining of HIF□2α in sections from trunk axial level of wild□type chick embryos at HH11, A, HH13, B, and HH18, C. Arrow denotes ventrally migrating HIF□2α positive cells. D, Co□immunostaining of HIF□2α and HNK1 (marker of migrating neural crest) in sections from trunk axial level of wild□type HH18 chick embryos. Arrows denote migrating cells double positive for the two proteins. E, Sections of HH13 wild□type embryo immunostained with DAPI for visualization of nuclei and secondary antibody only (donkey anti□rabbit Alexa Fluor□546). F, Western blot analysis for detection of HIF□2α protein at 21% and 1% O2 following siRNA mediated knockdown of HIF□1α or HIF□2α. DIP treated cells were used as a positive control and SDHA as loading control. Lanes between 21% and 1% siCTRL were removed from this figure, indicated by the black line. G, Immunohistochemical staining for HIF□2α in sections of SK□N□BE(2)c neuroblastoma cells cultured at 21% or 1% O2. H, Schematic of where oxygen measurements were performed. I, Oxygen saturation in the trunk of chick embryos during development measured ex ovo using microsensor technique. Error bars represent SEM, n ≥ 3 biologically independent replicates for each time point Image collected and cropped by CiteAb from the following open publication (https://pubmed.ncbi.nlm.nih.gov/32940375), licensed under a CC-BY license. Not internally tested by Novus Biologicals.

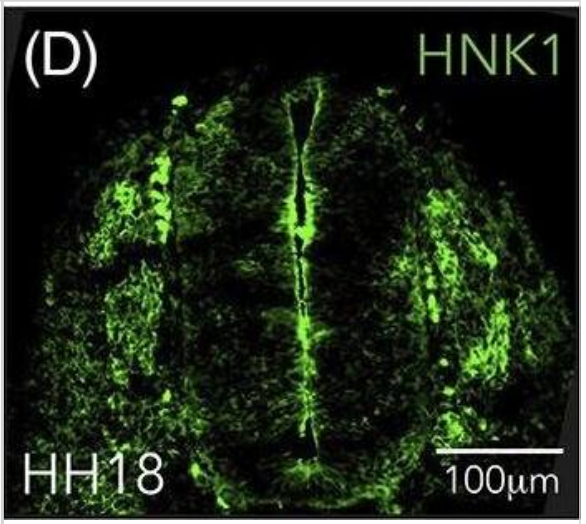

Publications

Nagati J, Dioum E, Giardinetto C et al. Select Early Growth Response (Egr) isoforms augment Hypoxia Inducible Factor 2 (HIF-2) regulation of erythropoietin (Epo) gene expression in mammals. The Journal of Biological Chemistry 2025-06-10 [PMID: 40505865]

Zhou X, Zheng Y, Sun W et al. D-mannose alleviates osteoarthritis progression by inhibiting chondrocyte ferroptosis in a HIF-2?-dependent manner Cell Proliferation 2021-11-01 [PMID: 34561933]

Liu S, Zhang G, Guo J et al. Loss of Phd2 cooperates with BRAFV600E to drive melanomagenesis Nat Commun 2018-12-21 [PMID: 30575721]

M Koeppen, JW Lee, SW Seo, KS Brodsky, S Kreth, IV Yang, PM Buttrick, T Eckle, HK Eltzschig Hypoxia-inducible factor 2-alpha-dependent induction of amphiregulin dampens myocardial ischemia-reperfusion injury Nat Commun, 2018-02-26;9(1):816. 2018-02-26 [PMID: 29483579]

R Berggren-N, M Ryde, A Löfdahl, A Ibáñez-Fon, M Kåredal, G Westergren, E Tufvesson, AK Larsson-Ca Effects of hypoxia on bronchial and alveolar epithelial cells linked to pathogenesis in chronic lung disorders Frontiers in Physiology, 2023-03-13;14(0):1094245. 2023-03-13 [PMID: 36994416]

Mallikarjuna P, Raviprakash TS, Aripaka K et al. Interactions between TGF-beta type I receptor and hypoxia-inducible factor-α mediates a synergistic crosstalk leading to poor prognosis for patients with clear cell renal cell carcinoma Cell Cycle 2019-09-01 [PMID: 31339433]

Kling L, Eulenberg-Gustavus C, Jerke U, Rousselle A et Al. ?(2)-integrins control HIF1? activation in human neutrophils Front Immunol 2024-10-29 [PMID: 39469705]

Xia J, Chen H, Wang X et Al. Sphingosine d18:1 promotes nonalcoholic steatohepatitis by inhibiting macrophage HIF-2? Nat Commun 2024-06-04 [PMID: 38834568]

Ivan Menendez-Montes, Beatriz Escobar, Manuel J. Gomez, Teresa Albendea-Gomez, Beatriz Palacios, Elena Bonzon-Kulichenko, Jose Luis Izquierdo-Garcia, Ana Vanessa Alonso, Alessia Ferrarini, Luis Jesus Jimenez-Borreguero, Jesus Ruiz-Cabello, Jesus Vázquez, Silvia Martin-Puig Activation of amino acid metabolic program in cardiac HIF1-alpha-deficient mice iScience 2021-02-03 [PMID: 33665549]

Hyunbum Kim, Yu Liu, Jiwon Kim, Yunhye Kim, Timothy Klouda, Sudeshna Fisch, Seung Han Baek, Tiffany Liu, Suzanne Dahlberg, Cheng-Jun Hu, Wen Tian, Xinguo Jiang, Kosmas Kosmas, Helen A Christou, Benjamin D Korman, Sara O Vargas, Joseph C Wu, Kurt R Stenmark, Vinicio de Jesus Perez, Mark R Nicolls, Benjamin A Raby, Ke Yuan Pericytes contribute to pulmonary vascular remodeling via HIF2α signaling EMBO Reports 2024-01-19 [PMID: 38243138]

Fan Y, Li H, Ma X et al. Dicer suppresses the malignant phenotype in VHL-deficient clear cell renal cell carcinoma by inhibiting HIF-2alpha. Oncotarget 2016-04-05 [PMID: 26943772]

Chul Ju Hwang, Mi Hee Park, Jae Yeon Hwang, Ju Hwan Kim, Na Young Yun, Sang Yeon Oh, Ju Kyung Song, Hyun Ok Seo, Yun-Bae Kim, Dae Yeon Hwang, Ki-Wan Oh, Sang-Bae Han, Jin Tae Hong CCR5 deficiency accelerates lipopolysaccharide-induced astrogliosis, amyloid-beta deposit and impaired memory function Oncotarget 2016-03-15 [PMID: 26910914]

More publications at http://www.novusbio.com/NB100-132

Procedures

Western Blot Protocol for HIF-2 alpha/EPAS1 Antibody (NB100-132)
Western Blot Protocol

1. Perform SDS-PAGE on samples to be analyzed, loading 10-25 ug of total protein per lane.
2. Transfer proteins to PVDF membrane according to the instructions provided by the manufacturer of the membrane and transfer apparatus.
3. Stain the membrane with Ponceau S (or similar product) to assess transfer success, and mark molecular weight standards where appropriate.
4. Rinse the blot TBS -0.05% Tween 20 (TBST).
5. Block the membrane in 5% Non-fat milk in TBST (blocking buffer) for at least 1 hour.
6. Wash the membrane in TBST three times for 10 minutes each.
7. Dilute primary antibody in blocking buffer and incubate overnight at 4C with gentle rocking.
8. Wash the membrane in TBST three times for 10 minutes each.
9. Incubate the membrane in diluted HRP conjugated secondary antibody in blocking buffer (as per manufacturer's instructions) for 1 hour at room temperature.
10. Wash the blot in TBST three times for 10 minutes each (this step can be repeated as required to reduce background).
11. Apply the detection reagent of choice in accordance with the manufacturer's instructions.

Novus Biologicals USA
10730 E. Briarwood Avenue
Centennial, CO 80112
USA
Phone: 303.730.1950
Toll Free: 1.888.506.6887
Fax: 303.730.1966
nb-customerservice@bio-techne.com

Bio-Techne Canada
21 Canmotor Ave
Toronto, ON M8Z 4E6
Canada
Phone: 905.827.6400
Toll Free: 855.668.8722
Fax: 905.827.6402
canada.inquires@bio-techne.com

Bio-Techne Ltd
19 Barton Lane
Abingdon Science Park
Abingdon, OX14 3NB, United Kingdom
Phone: (44) (0) 1235 529449
Free Phone: 0800 37 34 15
Fax: (44) (0) 1235 533420
info.EMEA@bio-techne.com

General Contact Information
www.novusbio.com
Technical Support: nb-technical@bio-techne.com
Orders: nb-customerservice@bio-techne.com
General: novus@novusbio.com

Products Related to NB100-132

NB820-59231	Human Kidney Whole Tissue Lysate (Adult Whole Normal)
NBP2-33376H	Blue Marker Antibody (6F4-F6) [HRP]
HAF007	Goat anti-Mouse IgG Secondary Antibody [HRP]
NB7539	Goat anti-Mouse IgG (H+L) Secondary Antibody [HRP]
NBP1-97005-0.5mg	Mouse IgG1 Isotype Control (MG1)

Limitations

This product is for research use only and is not approved for use in humans or in clinical diagnosis. Primary Antibodies are guaranteed for 1 year from date of receipt.

For more information on our 100% guarantee, please visit www.novusbio.com/guarantee

Earn gift cards/discounts by submitting a review: www.novusbio.com/reviews/submit/NB100-132

Earn gift cards/discounts by submitting a publication using this product: www.novusbio.com/publications